Two Pdk1 phosphorylation sites on the plant cell death suppressor Adi3 contribute to substrate phosphorylation

Joel W. Gray [a,1], Anna C. Nelson Dittrich [a,1,2], Sixue Chen [b], Julian Avila [a,3], Patrick Giavalisco [c], Timothy P. Devarenne [a,*]

[a] Department of Biochemistry and Biophysics, Texas A&M University, College Station, TX, 77843, USA
[b] Department of Biology, Genetics Institute, Plant Molecular and Cellular Biology Program, Interdisciplinary Center for Biotechnology Research, University of Florida, Gainesville, FL 32610, USA
[c] Max Planck Institute of Molecular Plant Physiology, 14476 Glom-Potsdam, Germany

ARTICLE INFO

ABSTRACT

The tomato AGC kinase Adi3 is phosphorylated by Pdk1 for activation of its cell death suppression activity. The Pdk1 phosphorylation site for activation of Adi3 is at Ser539. However, there is at least one additional Pdk1 phosphorylation site on Adi3 that has an unknown function. Here we identify an *Arabidopsis thaliana* sequence homologue of Adi3 termed AGC1-3. Two Pdk1 phosphorylation sites were identified on AGC1-3, activation site Ser596 and Ser269, and by homology Ser212 on Adi3 was identified as a second Pdk1 phosphorylation site. While Ser212 is not required for Adi3 autophosphorylation, Ser212 was shown to be required for full phosphorylation of the Adi3 substrate Gal83.

1. Introduction

The subfamily of eukaryotic protein kinases known as AGC kinases regulates a number of essential cellular processes such as protein expression, responses to stresses, and cell growth, survival, and death [1,2]. The name of this group of kinases is derived from three of its members, cAMP-dependent protein kinase 1 (PKA), cGMP-dependent protein kinase (PKG), and protein kinase C (PKC) [3]. In mammals, alterations in the regulation of, or mutations in AGC kinases are associated with several diseases including cancer [1]. 3-Phosphoinositide-dependent protein kinase 1 (Pdk1) is a member of the AGC kinases and is a master regulator of many AGC family members [1,4].

Activation and regulation of AGC kinases are governed by two main phosphorylation events. The first is the phosphorylation by Pdk1 of a Ser or Thr in the activation loop or T-loop [3]. Pdk1 phosphorylation

activates the AGC kinase and leads to further downstream phosphorylation of AGC substrates for regulation of the cellular processes associated with the particular AGC kinase [3,5]. The second phosphorylation event occurs on a Ser or Thr in a C-terminal hydrophobic motif known as the Pdk1 interacting fragment (PIF), and this event is carried out by a number of different kinases other than Pdk1 [1,6]. Pdk1 can bind the phosphorylated PIF through a domain termed the PIF binding pocket to allow for interaction with the AGC kinase substrate [1,6]. In plants, the AGC kinase PIF often contains an Asp or Glu that mimics the phosphorylation event for Pdk1 interaction [3,7]. The AGC kinases that are substrates of Pdk1 also contain a PIF binding pocket for self-binding of the PIF after activation by Pdk1, which helps stabilize the active conformation of the AGC kinase [6,8].

An additional phosphorylation site called the turn motif can be found on a subset of mammalian AGC kinases that are regulated by growth factors [1,9]. As with the PIF, the turn motif is C-terminal, but is upstream of the PIF phosphorylation site [9]. The kinase(s) that phosphorylates the turn motif has yet to be identified. But, the role of turn motif phosphorylation has been shown to stabilize the active conformation of the AGC kinase, prevent PIF dephosphorylation [1,9], and in the case of PRK2 inhibit interaction with Pdk1 [10].

In plants, the phosphorylation state of AGC kinases is much less clear. Several studies have shown that AGC kinases from plants are phosphorylated by Pdk1 for activation [4,7,11–13]. But, the presence of additional phosphorylation sites on the AGC kinase required for activation or conformation stabilization is lacking. Our previous studies

---

have shown that the tomato (*Solanum lycopersicum*; *Sl*) AGC kinase Adi3 is phosphorylated by SlPdk1 at Ser539, and this phosphorylation event is required for activation of the cell death suppression activity of Adi3 [7,14]. These studies also showed that there is at least one additional *Sl*Pdk1 phosphorylation site on Adi3 [7]. We have examined Adi3 for a turn motif-like site, but there does not appear to be one present (data not shown). Thus, the identity of this additional phosphorylation site(s) or role in Adi3 function has been unknown. Here we report the identification of a second *Sl*Pdk1 phosphorylation site on Adi3 through comparative studies with the *Arabidopsis thaliana* sequence homologue of Adi3, AGC1-3, and mass spectrometry. This second Adi3 phosphorylation site appears to be required for full activation of kinase activity toward substrates.

2. Materials and methods

2.1. Cloning, expression, purification, and mutagenesis of Adi3, AGC1-3, Gal83, SlPdk1, and AtPdk1

Cloning of the Adi3, *Sl*Pdk1, and Gal83 cDNAs into pMAL-c2 and expression/purification of protein from *Escherichia coli* for N-terminal maltose binding protein (MBP) translational fusions were previously described [7,15]. Site-directed mutagenesis was carried out using standard protocols and Pfu Turbo DNA polymerase (Stratagene). All primers used in this study for cloning and mutagenesis are listed in Supplemental Table 1.

The *Arabidopsis thaliana* sequence homolog to Adi3, AGC1-3 (At2g44830; accession # AY078927), was identified by BLAST of the *Arabidopsis* genome (www.arabidopsis.org) using the full-length open reading frame (ORF) sequence of Adi3. The 2298 bp full-length ORF of AGC1-3 was cloned by RT-PCR. Total mRNA was extracted from *Arabidopsis* (Col-0) leaf tissue and first strand synthesis was completed with the SuperScriptII cDNA synthesis kit (Invitrogen). The AGC1-3 ORF was amplified from first strand cDNA with primers based at the ATG start codon and the TAA stop codon using GoTaq Green (Promega). The product was cloned into pCR2.1-TOPO (Invitrogen) to confirm identity by sequencing. All AGC1-3 variants (full-length and N-terminal deletions) were cloned into a modified form of pET41a (Novagen), which expresses MBP-fusions rather than GST-fusion proteins. This modified pET41a was created by digestion with *Nde*I and *Spe*I to remove the GST ORF and cloning of the MBP ORF, amplified from pMAL-C2, into the same sites. Expression and purification of MBP-AGC1-3 fusion proteins expressed from the modified pET41a yielded higher protein levels compared to pMAL-C2, possibly due to the longer linker region between MBP and AGC1-3 in the modified pET41a compared to pMAL-C2. All variants of AGC1-3 used in this study were cloned into the 5′ *Eco*RI and 3′ *Xho*I sites of the modified pET41a vector, and the yeast 2-hybrid plasmids pEG202 and pJG4-5.

The *At*Pdk1-1 cDNA (At5g04510; accession # NM_203001) has been previously described [16]. The full length *At*Pdk1-1 ORF was amplified from first strand cDNA and cloned into pCR2.1-TOPO as with AGC1-3. The *At*Pdk1-1 ORF was subcloned into the *Eco*RI and *Xho*I sites of the bacterial expression vectors pGEX (Amersham Biosciences) and pMAL-c2, and the yeast 2-hybrid plasmids pEG202 & pJG4-5.

2.2. Mass spectrometry

For MS analysis of Adi3 phosphorylation sites, 5 μg of MBP-Adi3 was phosphorylated by 1 μg MBP-*Sl*Pdk1 in an in vitro kinase assay and samples separated by 10% SDS-PAGE as detailed below for kinase assays, except non-radiolabeled ATP was used. For sample preparation, coomassie stained gel bands were in-gel digested with trypsin overnight [17] and phosphopeptides were enriched using a NuTip metal oxide phosphoprotein enrichment kit according to manufacturer's instructions (Glygen, Columbia, MD).

For LC–MS/MS analysis, phosphopeptides were injected onto a capillary trap (LC Packings PepMap, Amsterdam, Netherlands) and desalted for 5 min with 0.1% v/v acetic acid at a flow rate of 3 μl/min. The samples were loaded onto an LC Packings C_{18} PepMap nanoflow HPLC column. The elution gradient of the HPLC column started at 97% solvent A, 3% solvent B and finished at 60% solvent A, 40% solvent B for 30 min. Solvent A consisted of 0.1% v/v acetic acid, 3% v/v ACN, and 96.9% v/v H_2O. Solvent B consisted of 0.1% v/v acetic acid, 96.9% v/v ACN, and 3% v/v H_2O. LC–MS/MS analysis was carried out on a LTQ Orbitrap XL mass spectrometer (Thermo Scientific, Bremen, Germany). The instrument under Xcalibur 2.07 with LTQ Orbitrap Tune Plus 2.55 software was operated in the data dependent mode to automatically switch between MS and MS/MS acquisition. Survey scan MS spectra (from m/z 300–2000) were acquired in the orbitrap with resolution R = 60,000 at m/z 400. During collisionally induced dissociation (CID), if a phosphate neutral loss of 98, 49, 32.66 and 24.5 m/z below the precursor ion mass was detected, there was an additional activation of all four neutral loss m/z values. This multistage activation was repeated for the top five ions in a data-dependent manner. Dynamic exclusion was set to 60 s. Typical mass spectrometric conditions include a spray voltage of 2.2 kV, no sheath and auxiliary gas flow, a heated capillary temperature of 200 °C, a capillary voltage of 44 V, a tube lens voltage of 165 V, an ion isolation width of 1.0 m/z, and a normalized CID collision energy of 35% for MS/MS in LTQ. The ion selection threshold was 500 counts for MS/MS. The mass spectrometer calibration was performed according to the manufacturer's guidelines using a mixture of sodium dodecyl sulfate, sodium taurocholate, MRFA and Ultramark.

For the protein search algorithm, all MS/MS spectra were analyzed using Mascot (Matrix Science, London, UK; version 2.4). Mascot was set up to search a current *Arabidopsis* database assuming the digestion enzyme trypsin and one miscleavage. Mascot was searched with a fragment ion mass tolerance of 0.80 Da and a parent ion tolerance of 10 ppm. Iodoacetamide derivative of Cys, deamidation of Asn and Gln, oxidation of Met and phosphorylation of serine, threonine and tyrosine are specified as variable modifications. The MS/MS spectra of the identified phosphorylated peptides were manually inspected to ensure confidence in phosphorylation site assignment.

2.3. Yeast two-hybrid assay

Y2H assays were conducted using pEG202 for the bait vector and pJG4-5 for the prey vector as described previously [7]. Constructs were transformed into yeast strain EGY48 containing the pSH18-34 reporter vector and analyzed for *LacZ* gene expression on 5-bromo-4-chloro-3-indolyl-β-D- galactopyranoside-containing plates. Protein expression was confirmed by Western blot. All other procedures for the Y2H assays followed standard procedures as described previously [18].

2.4. Kinase assays

In vitro kinase assays were done in 30 μl reactions in kinase buffer (10 mM Tris–HCl, pH 7.5, 10 mM $MgCl_2$, 1 mM dithiothreitol [DTT]) with the protein amounts given in the figure legends. The reactions were started by the addition of 0.25 μCi of [γ-^{32}P]ATP (6000 Ci mmol^{-1}; Perkin-Elmer) and non-radiolabeled ATP to a final concentration of 20 μM per sample followed by incubation for 30 min at 30 °C. Reactions were terminated by the addition of 4× SDS-PAGE sample buffer, and samples were resolved by 10% SDS-PAGE or 1:200 bis-acrylamide:acrylamide 10% SDS-PAGE (see below). Visualization and quantification of incorporated radioactivity were done using a phosphorimager (Bio-Rad Molecular Imager) and quantification software (Bio-Rad Quantity One). For non-radioactive kinase assays (Fig. 4C), the assays were carried out as above with the omission of [γ-^{32}P]ATP. The kinase artificial substrate myelin basic protein was purchased from Sigma.

2.5. Pull-down assays

For MBP-AGC1-3 and GST-AtPdk1-1 pull-down assays, cell pellets from 2 ml cultures were lysed by sonication in 500 μl of extraction buffer (50 mM Tris, pH 8.0, 50 mM NaCl, 5 mM EDTA, 0.1% Triton X-100, 1× general protease inhibitors [Sigma]) and cell debris pelleted by centrifugation at 5000 ×g, 4 °C for 5 min. One hundred μg of the supernatant (total protein) from each extract was added to 50 μl of equilibrated amylose resin, the volume adjusted to 1 ml with extraction buffer, incubated on a nutator at 4 °C for 30 min, the resin pelleted by centrifugation at 1000 ×g for 1 min, and the resin washed 3 times with 500 μl of extraction buffer. Samples were eluted from the resin with 100 μl of 1× SDS-PAGE buffer at 95 °C for 5 min, and 5 μl of each sample was analyzed by 10% SDS-PAGE. Proteins were analyzed by Western blotting using α-GST (Santa Cruz Biotechnology) at 1:4000 or α-MBP (New England BioLabs) at 1:10,000.

2.6. 1:200 bis-acrylamide:acrylamide SDS-PAGE

10% SDS-PAGE gels with a 1:200 bis-acrylamide:acrylamide ratio were made by mixing the following: 2.5 ml 4× resolving gel buffer (1.5 M Tris-base, 0.4% SDS, pH 8.8), 3.317 ml 30% acrylamide, 250 μl 2% bis-acrylamide, 50 μl 10% ammonium persulfate, and 5 μl N, N, N′, N′-tetramethylethylenediamine (TEMED) in a final volume of 10 ml. These gels were used with a typical 4% acrylamide stacking gel. Gels were run at 150 V for approximately 4 h.

2.7. λ phosphatase treatment

Adi3 and SlPdk1 were incubated in a 30 μl in vitro kinase assay as described above with only non-radiolabeled ATP. Following the kinase assay 4 μl of 10× λ phosphatase buffer (500 mM HEPES, pH 7.5, 1 M NaCl, 20 mM DTT, 0.1% Brij 35) and 4 μl of 10 mM MnCl$_2$ were added for a final volume of 38 μl. Reactions were started with the addition of 800 units (2 μl) of λ phosphatase (New England Biolabs), incubated at 30 °C for 1 h, and reactions were terminated by the addition of 10 μl 4× SDS-PAGE sample buffer. Samples were then resolved by 1:200 bis-acrylamide:acrylamide 10% SDS-PAGE as described above.

3. Results

3.1. Mass spectrometry analysis of SlPdk1 phosphorylated Adi3

From our previous studies we have shown that SlPdk1 phosphorylates Adi3 only on Ser residues, phosphorylation of Ser539 accounts for ~40–50% of SlPdk1 activity on Adi3, and at least one additional Adi3 Ser residue accounts for the remaining phosphorylation by SlPdk1 [7]. In an effort to identify the additional SlPdk1 phosphorylation site(s) on Adi3 we initially took a mass spectrometry (MS) approach. Kinase-inactive Adi3^{K337Q} was phosphorylated by SlPdk1 using non-radiolabeled ATP, digested with trypsin, and analyzed by tandem MS/MS, which identified 20 peptides giving 49% coverage of the Adi3 protein sequence (Supplemental Fig. 1). This MS/MS analysis was repeated several times without an increase in peptide coverage of Adi3. Two new phosphorylated Ser residues were found in two separate Adi3 peptides; Ser119 and Ser518 (Supplemental Figs. 1–3). The previously identified SlPdk1 phosphorylation activation site in Adi3, Ser539 [7], was also identified as a phosphorylated residue (Supplemental Figs. 1, 4).

3.2. The MS/MS-identified phosphorylation sites do not contribute to SlPdk1 phosphorylation of Adi3 or Adi3 auto- or trans-phosphorylation

In order to confirm or deny that the phosphorylated Adi3 Ser residues identified by MS/MS were phosphorylated by SlPdk1, each residue was
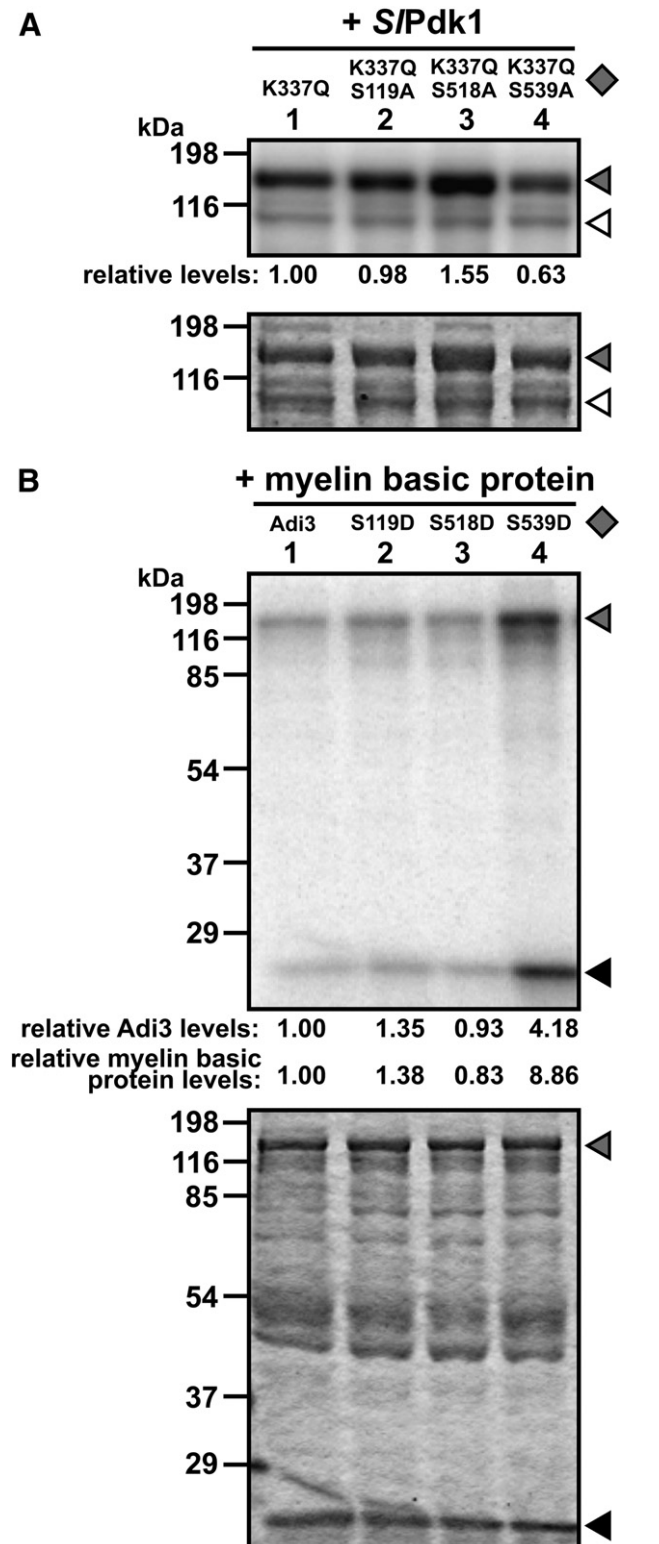
Fig. 1. Contribution of MS/MS-identified Adi3 phosphorylation sites to phosphorylation by SlPdk1 and Adi3 trans-phosphorylation. In (A) and (B), the indicated proteins were incubated in an in vitro kinase assay with γ-[^{32}P]ATP. Top panel, phosphorimage; bottom panel, coomassie stained gel. Relative values of phosphorylation are given below each lane and are representative of two independent experiments. Gray diamond, form of MBP-Adi3 used in assay. Gray, open, and black triangles, location of MBP-Adi3, MBP-SlPdk1, and myelin basic protein, respectively. The following amounts of each protein were used in the assay: MPB-Adi3, 5 μg; MBP-SlPdk1, 1.0 μg; myelin basic protein, 5 μg. (A) Ala mutation of the identified phosphorylated Ser residues does not reduce SlPdk1 phosphorylation of Adi3. (B) Asp mutation of the identified phosphorylated Ser residues does not increase Adi3 phosphorylation of myelin basic protein.

mutated to Ala in the kinase-inactive Adi3^{K337Q} background, the proteins incubated with *Sl*Pdk1 in an in vitro kinase assay with [γ-^{32}P]ATP, and the level of Adi3 phosphorylation quantified and compared to the level of phosphorylation for Adi3^{K337Q}. As we have seen previously [7], the S539A mutation reduces *Sl*Pdk1 phosphorylation of Adi3 by ~40% (Fig. 1A, Lane 4). However, the Ala mutations of the other Ser residues identified here by MS/MS did not reduce *Sl*Pdk1 phosphorylation of Adi3 and in some cases even increased phosphorylation (Fig. 1A, Lanes 2, 3).

We have previously shown that mutation of Adi3 Ser539 to the phosphomimetic Asp greatly increases autophosphorylation and substrate phosphorylation [7,14,15] supporting activation of Adi3 by *Sl*Pdk1 phosphorylation of this site. Next, we mutated the MS/MS-identified phosphorylation sites to Asp and tested autophosphorylation as well as phosphorylation of the protein kinase artificial substrate myelin basic protein. As we have seen before, the S539D mutation greatly increases Adi3 auto- and *trans*-phosphorylation (Fig. 1B, Lane 4). The S119D, mutation increased Adi3 autophosphorylation only slightly above that of wild-type and not to the extent of S539D (Fig. 1B, Lane 2), while S518D was slightly lower than wild-type (Fig. 1B, Lane 3). Similar results were seen for phosphorylation of myelin basic protein by the Asp mutations; only the S539D mutation greatly increased the phosphorylation of the substrate (Fig. 1B, lane 4). These results may suggest that Ser119 and

Ser518 are not bona fide *Sl*Pdk1 phosphorylation sites and may be artifacts of the in vitro kinase assay. These residues are most likely not Adi3 autophosphorylation sites since the kinase-inactive Adi3^{K337Q} was used for the MS/MS analysis.

3.3. Identification and characterization of AGC1-3, the Arabidopsis thaliana sequence homologue of Adi3

At the same time we were carrying out the MS/MS analysis and characterization of the identified Adi3 phosphorylation sites described above, we began to characterize the *Arabidopsis thaliana* sequence homologue of Adi3 to identify *Arabidopsis thaliana* Pdk1 (*At*Pdk1) phosphorylation sites. A BLAST search of the *Arabidopsis* genome and proteome using the Adi3 cDNA and protein sequences returned gene At2g44830 (a.k.a. AGC1-3 [3]) as the closest sequence homologue to Adi3. A comparison of AGC1-3 to Adi3 shows that they share 63.8% amino acid identity and have the same protein domains that are the hallmarks of the VIIIa group of plant AGC kinases such as a PIF, PIF binding pocket, kinase domain, and T-loop extension (Fig. 2A; Supplemental Fig. 5). AGC1-3 is 65 amino acids longer than Adi3, which is mainly localized to the region N-terminal to the kinase domain (Fig. 2A; Supplemental Fig. 5).
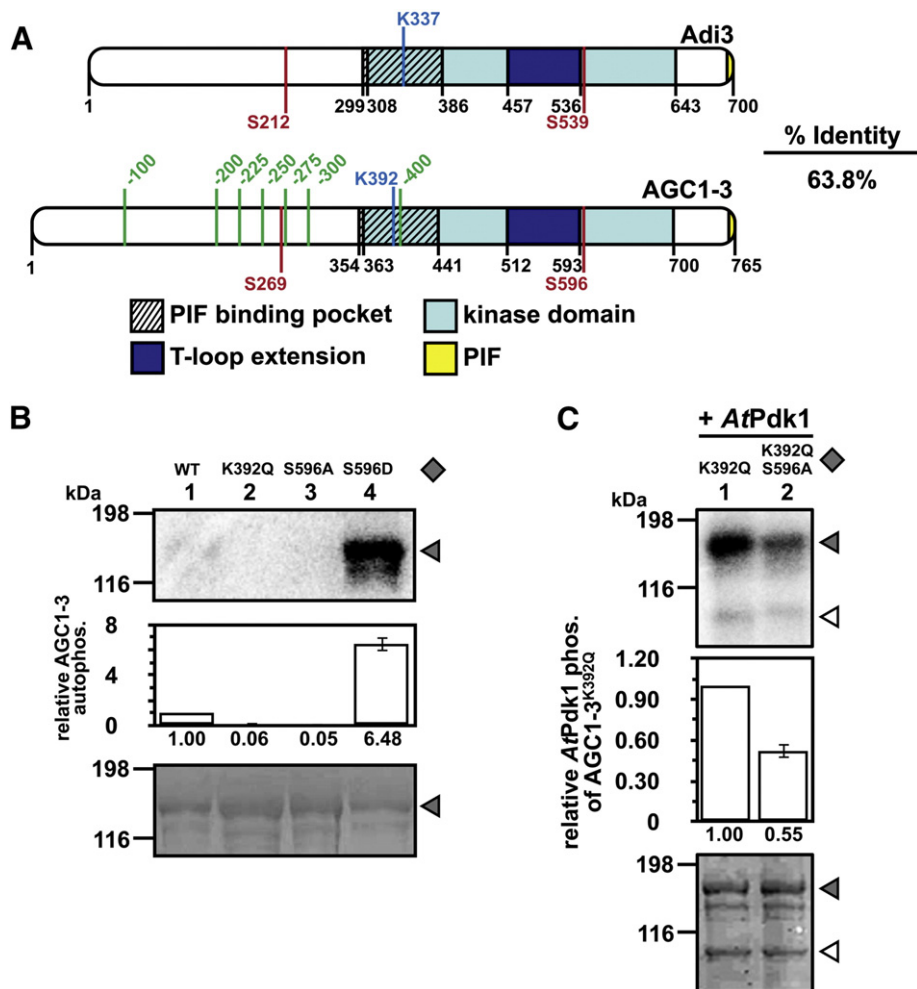
Fig. 2. Protein domains, autophosphorylation, and *At*Pdk1 phosphorylation of AGC1-3. (A) Protein domain alignment of Adi3 and AGC1-3 (At2g44830). Amino acid positions for domains are in black, phosphorylation sites are in red, and N-terminal truncation sites for the assay in Fig. 3A are in green. In (B) and (C), the indicated MBP-AGC1-3 proteins were incubated in an in vitro kinase assay with γ-[^{32}P]ATP. Top panel, phosphorimage; bottom panel, coomassie stained gel; middle panel, quantification of AGC1-3 autophosphorylation (B) or phosphorylation by *At*Pdk1 (C) from at least 3 independent assays. Error bars indicate standard error. Average value is shown under each column. Gray diamond, form of MBP-AGC1-3 used in assay. Gray and open triangles, location of MBP-AGC1-3 and GST-*At*Pdk1, respectively. The following amounts of each protein were used in the assay: MPB-AGC1-3, 8 μg, GST-*At*Pdk1, 4 μg. (B) AGC1-3 encodes a functional protein kinase. Analysis of wild-type, kinase-deficient, and constitutively active MBP-AGC1-3 fusion proteins by in vitro autophosphorylation assays. (C) Ser596 accounts for 45% of *At*Pdk1 phosphorylation of AGC1-3. Analysis of *At*Pdk1 phosphorylation of AGC1-3 in in vitro kinase assays.

There have been minimal studies on AGC1-3. The only experimental characterization of AGC1-3 has shown that it is a phosphorylation substrate of *At*Pdk1 and that its mRNA is expressed in seedlings, reproductive organs (inflorescences, flowers, siliques), and roots [4]. Interestingly, AGC1-3 is not expressed in cauline leaves or stems of mature plants [4]. We have shown that AGC1-3 and *At*Pdk1 interact in a yeast two-hybrid (Y2H) assay in reciprocal combinations of the proteins as bait and prey (Supplemental Fig. 6, samples 2, 3) and that this interaction was dependent on the presence of the AGC1-3 PIF motif (Supplemental Fig. 6, sample 12).

We next tested the autophosphorylation activity of AGC1-3 using in vitro kinase assays. Wild-type AGC1-3 showed a low level of autophosphorylation activity (Fig. 2B, Lane 1), whereas AGC1-3^{K392Q}, which has a mutation in the Lys residue that corresponds to the Lys337 ATP-binding residue in Adi3 (Fig. 2A; Supplemental Fig. 5), did not (Fig. 2B, Lane 2). Serine 596 corresponds to the conserved Pdk1 phosphorylation site in the activation loop of AGC1-3 and mutation to Ala (S596A) eliminated AGC1-3 autophosphorylation (Fig. 2B, Lane 3), while mutation to Asp (S596D) greatly increased this activity (Fig. 2B, Lane 4). This would suggest that phosphorylation of Ser596 contributes to full activity of AGC1-3.

Even though AGC1-3 has been shown to be phosphorylated by *At*Pdk1 [4], the actual site(s) of phosphorylation was not identified. Thus, we tested the contribution of Ser596 to *At*Pdk1 phosphorylation of AGC1-3. Using the kinase deficient AGC1-3^{K392Q} it was seen that *At*Pdk1 can phosphorylate AGC1-3 (Fig. 2C, lane 1) and the Ala mutation of Ser596 in the AGC1-3^{K392Q} background resulted in a loss of ~45% of the *At*Pdk1 phosphorylation of AGC1-3 (Fig. 2C, Lane 2). Both of the AGC1-3^{K392Q} and AGC1-3^{S596A} proteins maintain interaction with *At*Pdk1 (Supplemental Fig. 6, samples 4, 5). This data would suggest that Ser596 is an *At*Pdk1 phosphorylation site in AGC1-3.

3.4. N-terminal truncations of AGC1-3 identify Ser269 as a second AtPdk1 phosphorylation site

Since MS/MS on *Sl*Pdk1 phosphorylated Adi3 was not successful in identifying additional phosphorylation sites, we took the alternate approach with AGC1-3 of using truncations to identify additional *At*Pdk1 phosphorylation sites. Successive AGC1-3 100 amino acid N-terminal deletions up to 400 amino acids, as shown in Fig. 2A, were constructed in the kinase-inactive AGC1-3$^{K392Q/S596A}$ background and tested for phosphorylation by *At*Pdk1. After deletion of the first AGC1-3 100 amino acids, phosphorylation by *At*Pdk1 increased over that of the full length protein (Fig. 3A, Lanes 1, 2) suggesting an inhibitory function for these first 100 AGC1-3 amino acids for interaction with or phosphorylation by *At*Pdk1. The AGC1-3$^{\Delta200}$ deletion protein did not change the phosphorylation by *At*Pdk1 compared to AGC1-3$^{\Delta100}$ (Fig. 3A, Lane 3). However, the AGC1-3$^{\Delta300}$ deletion caused a drastic decrease in the phosphorylation of AGC1-3 by *At*Pdk1 (Fig. 3A, Lane 4), as did the AGC1-3$^{\Delta400}$ deletion (Fig. 3A, Lane 5), suggesting that an additional *At*Pdk1 phosphorylation site(s) in AGC1-3 exists between amino acids 200 and 300. This was confirmed by creating further AGC1-3 N-terminal truncations of 25 amino acids based on the AGC1-3$^{\Delta200/K392Q/S596A}$ protein and testing these proteins for *At*Pdk1 phosphorylation. The AGC1-3$^{\Delta275}$ protein had a large reduction in *At*Pdk1 phosphorylation indicating a second *At*Pdk1 phosphorylation site in AGC1-3 exists between amino acids 250 and 275. The reduction in *At*Pdk1 phosphorylation of the AGC1-3 N-terminal deletions was not due to a reduced interaction with *At*Pdk1 since all the AGC1-3 N-terminal deletions were capable of pulling down equal amounts of *At*Pdk1 (Supplemental Fig. 7). There are eight Ser residues within this amino acid 250 to 275 region of AGC1-3. However, only one Ser, Ser269, has a similar surrounding sequence as the Ser596 activation loop *At*Pdk1 site (Fig. 3B).
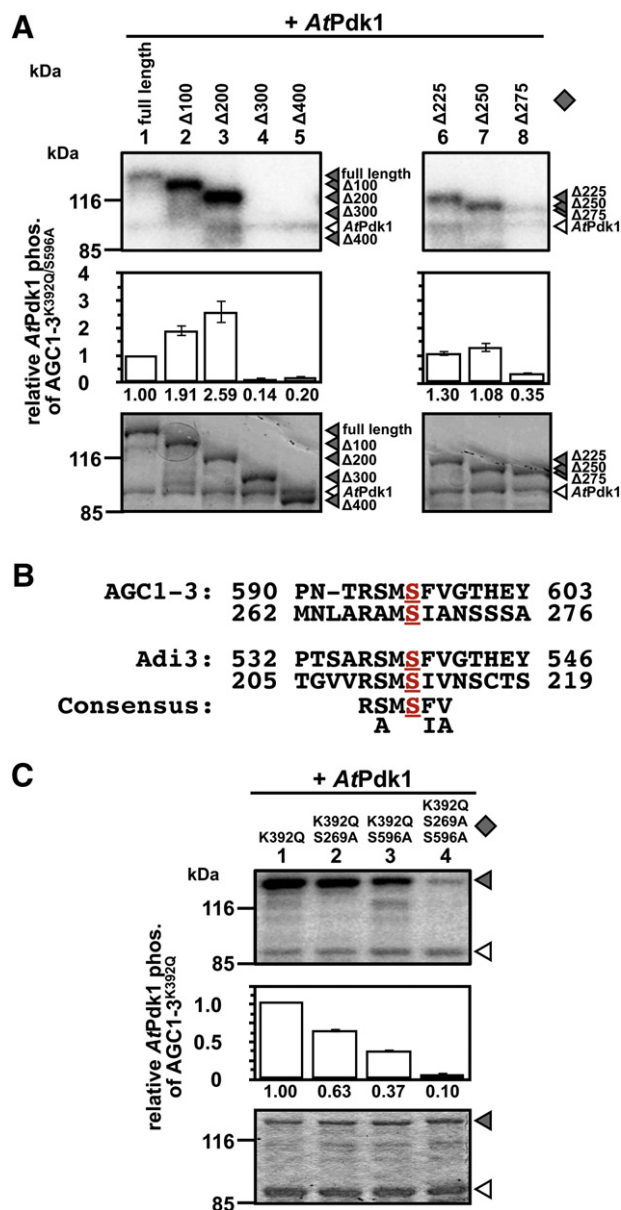
Fig. 3. Identification of Ser269 as a second phosphorylation site in AGC1-3. In A and C, the indicated proteins were incubated in an in vitro kinase assay with γ-[^{32}P]ATP. Top panel, phosphorimage; bottom panel, coomassie stained gel; middle panel, quantification of AGC1-3 phosphorylation by *At*Pdk1 from at least 3 independent assays. Average value is shown under each column. Error bars indicate standard error. Gray diamond, form of MBP-AGC1-3 used in assay. Gray triangles, location of MBP-AGC1-3$^{K392Q/S595A}$ N-terminal truncation (B) and MBP-AGC1-3 (C) proteins. Open triangles, location of MBP-*At*Pdk1. The following amounts of each protein were used in the assay: MBP-*At*Pdk1, 4 μg; MPB-AGC1-3, 5 μg. (A) Identification of AGC1-3 Ser269 phosphorylation by *At*Pdk1 using kinase inactive N-terminally truncated MBP-AGC1-3$^{K392Q/S596A}$ proteins. (B) Amino acid sequences around the conserved Pdk1 phosphorylation sites in AGC1-3 (S596) and Adi3 (S539), the identified second Pdk1 phosphorylation site in AGC1-3 (S269), the homologous site in Adi3 (S212), and the consensus sequence. (C) MBP-*At*Pdk1 phosphorylation of MBP-AGC1-3 kinase site mutants produced in the kinase inactive K392Q background.

In order to confirm Ser269 as an *At*Pdk1 phosphorylation site on AGC1-3, this amino acid was mutated to Ala in the AGC1-3^{K392Q} and AGC1-3$^{K392Q/S596A}$ backgrounds and tested for phosphorylation by *At*Pdk1. These proteins did not contain autophosphorylation activity (Supplemental Fig. 8A) indicating that any phosphorylation when incubated with *At*Pdk1 could be attributed to *At*Pdk1. The *At*Pdk1 phosphorylation of AGC1-3$^{K392Q/S269A}$ was reduced by ~40% compared to AGC1-3^{K392Q} (Fig. 3C, compare Lanes 1, 2) and the double phosphorylation site mutant AGC1-3$^{K392Q/S596A/S269A}$ showed a large

~90% decrease in *At*Pdk1 phosphorylation (Fig. 3C, Lane 4). These data suggest that both Ser269 and Ser539 are the main *At*Pdk1 phosphorylation sites in AGC1-3, and there may be additional minor phosphorylation sites.

3.5. Adi3 Ser212 is homologous to AGC1-3 Ser269 and is a second SlPdk1 phosphorylation site

We next used the data obtained for the AGC1-3 Ser269 *At*Pdk1 phosphorylation site to identify a potential second *Sl*Pdk1 site in Adi3. An alignment of the Adi3 and AGC1-3 protein sequence shows that Ser212 of Adi3 aligns with that of AGC1-3 Ser269 (Fig. 3B; Supplemental Fig. 5). As with AGC1-3 Ser269, the sequence surrounding Adi3 Ser212 is similar to that around the conserved Ser539 activation loop *Sl*Pdk1 site (Fig. 3B) suggesting this may be an *Sl*Pdk1 phosphorylation site.

The contribution of Ser212 toward *Sl*Pdk1 phosphorylation of Adi3 was tested using in vitro kinase assays. As with AGC1-3 Ser269, Ser212 was mutated to Ala in the kinase-inactive Adi3^{K337Q} and Adi3$^{K337Q/S539A}$ backgrounds and tested for phosphorylation by *Sl*Pdk1. These proteins did not contain autophosphorylation activity (Supplemental Fig. 8B) indicating that any phosphorylation when incubated with *Sl*Pdk1 could be attributed to *Sl*Pdk1. The *Sl*Pdk1 phosphorylation of Adi3$^{K337Q/S212A}$ was reduced by ~40% compared to Adi3^{K337Q} (Fig. 4A, compare Lanes 1, 2) and the double phosphorylation site mutant Adi3$^{K337Q/S212A/S539A}$ showed an ~74% reduction in *Sl*Pdk1 phosphorylation (Fig. 4A, Lane 4).

Since we have previously shown that the Adi3^{S539D} phosphomimetic protein has increased autophosphorylation [7], the Adi3^{S212D} phosphomimetic protein was analyzed for increased autophosphorylation. The Adi3^{S212D} protein did not have increased autophosphorylation over that of wild-type protein (Fig. 4B, Lanes 1, 2) and introducing the S212D mutation into the Adi3^{S539D} background did not increase autophosphorylation over that of the Adi3^{S539D} protein alone (Fig. 4B, Lanes 3, 4). These data suggest that both Ser212 and Ser539 are *Sl*Pdk1 phosphorylation sites in Adi3, there is an additional site(s) since there is still 10% of *Sl*Pdk1 phosphorylation remaining in the Adi3$^{K337Q/S539A/S296A}$ protein, and that phosphorylation of Ser212 does not contribute to Adi3 autophosphorylation.

As additional evidence that Ser212 is an *Sl*Pdk1 phosphorylation site on Adi3 we analyzed *Sl*Pdk1 phosphorylated Adi3 proteins by SDS-PAGE for the identification of Adi3 protein band shifts due to phosphorylation. The SDS-PAGE gels used in these assays contain a *bis*-acrylamide:acrylamide ratio of 1:200 rather than the standard 1:37.5 ratio. Studies from our lab and others have shown that the 1:200 gels are capable of efficiently separating phosphoproteins based on single phosphorylation events [15,19]. Adi3 proteins with the non-phosphorylatable S212A and S539A mutations in the kinase-inactive Adi3^{K337Q} background were phosphorylated by *Sl*Pdk1 and separated by 1:200 10% SDS-PAGE. The non-*Sl*Pdk1 phosphorylated proteins appeared as single protein bands (Fig. 4C, Lanes 1–4), while the *Sl*Pdk1 phosphorylated proteins were separated into several different protein bands (Fig. 4C, Lanes 6–9). The Adi3^{K337Q} protein appeared as three distinct protein bands (Fig. 4C, Lane 6), the Adi3$^{K337Q/S212A}$ and Adi3$^{K337Q/S539A}$ proteins appeared as two distinct protein bands (Fig. 4C, Lanes 7, 8), and the Adi3$^{K337Q/S212A/S539A}$ protein appeared as a single protein band (Fig. 4C, Lane 9). This would suggest that Adi3 exists in three different
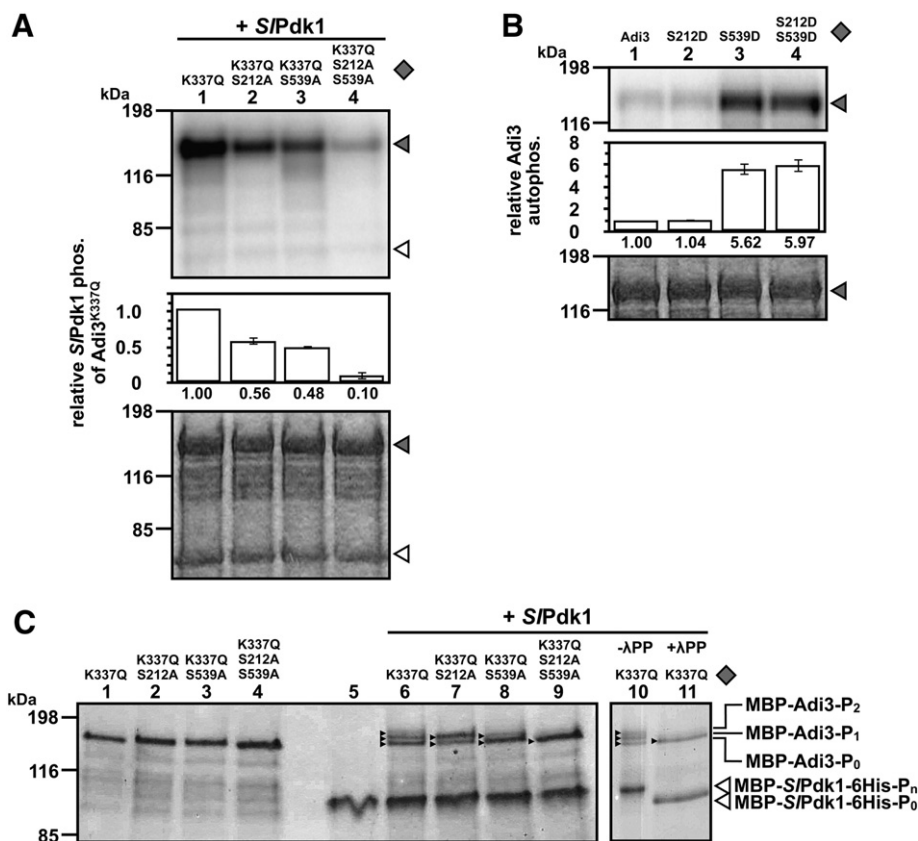
Fig. 4. Evidence for Adi3 Ser212 phosphorylation by *Sl*Pdk1. In A and B, the indicated proteins were incubated in an in vitro kinase assay with γ-[^{32}P]ATP. Top panel, phosphorimage; bottom panel, coomassie stained gel; middle panel, quantification of Adi3 autophosphorylation (A) or *Sl*Pdk1 phosphorylation of Adi3 (B) from at least 3 independent assays. Average value is shown under each column. Error bars indicate standard error. Gray diamond, form of MBP-Adi3 used in assay. Gray and open triangles, location of MBP-Adi3 and *Sl*Pdk1-6His (A) or MBP-*Sl*Pdk1-6His (C), respectively. The following amounts of each protein were used in the assay: MPB-Adi3, 5 μg; MBP-*Sl*Pdk1-6His, 0.5 μg. (A) Adi3 Ser212 is phosphorylated by *Sl*Pdk1. (B) Ser212 does not contribute to Adi3 autophosphorylation. (C) Separation of *Sl*Pdk1-phosphorylated Adi3. The indicated proteins were incubated in an in vitro kinase assay with non-radiolabeled ATP followed by SDS-PAGE using a 1:200 ratio of *bis*-acrylamide:acrylamide and stained with coomassie. Different phosphorylated species of Adi3 are indicated by black arrowheads next to the band. 2 μg of both MBP-Adi3 and MBP-*Sl*Pdk1-6His was used in the assay.

*Sl*Pdk1 phosphorylated forms and each Adi3 protein band corresponds to a phosphoprotein from *Sl*Pdk1 phosphorylation. The protein band seen in Adi3$^{K337Q/S2121A/S539A}$ presumably contains a minor amount of *Sl*Pdk1 phosphorylation since this protein still contains 10% of *Sl*Pdk1 phosphorylation (Fig. 4A). In order to confirm these Adi3 bands as phosphoproteins, we treated *Sl*Pdk1 phosphorylated Adi3^{K337Q} with λ phosphatase to remove phosphate groups and analyzed by 1:200 10% SDS-PAGE. As seen previously, *Sl*Pdk1 phosphorylated Adi3^{K337Q} appeared as three distinct protein bands (Fig. 4C, Lane 10). Treatment with λ phosphatase reduced Adi3^{K337Q} to a single protein band (Fig. 4C, Lane 11). Taken together, these data indicate the two slower migrating Adi3 bands are due to phosphorylation at Ser212 and Ser539, while the fastest migrating protein should contain a minimal amount of *Sl*Pdk1 phosphorylation. λ phosphatase treatment also shifted the migration of *Sl*Pdk1 (Fig. 4C, compare Lanes 10, 11) indicating it is also phosphorylated in the assay. Interestingly, *Sl*Pdk1 did not appear as multiple phosphoprotein bands without λ phosphatase (Fig. 4C, Lane 10) suggesting a single phosphorylation state for *Sl*Pdk1.

For a final piece of evidence that Ser212 is phosphorylated in Adi3 by *Sl*Pdk1 we repeated MS/MS on *Sl*Pdk1 phosphorylated Adi3^{K337Q} followed by LC–MS/MS analysis on an LTQ-Orbitrap mass spectrometer system as we previously reported [15]. This analysis positively identified Ser212 phosphorylation (Supplemental Fig. 9), and altogether the data presented indicate that Ser212 is a second *Sl*Pdk1 phosphorylation site on Adi3.

3.6. The phosphomimetic mutation of Ser212 and Ser539 contributes to full Adi3 phosphorylation of Gal83

Since the phosphomimetic proteins Adi3^{S212D} or Adi3$^{S212D/S539D}$ did not affect Adi3 autophosphorylation, we analyzed the contribution of Ser212 toward phosphorylation of an Adi3 substrate. We have previously shown that Adi3 phosphorylates Gal83, the β-subunit of the tomato SnRK1 protein complex, at Ser26 [15,20]. The SnRK1 protein complex regulates metabolism under numerous situations including resistance to pathogens [21,22], and the β-subunits of this complex control cell localization, substrate specificity, and complex activity [23–26]. We have shown that Adi3 phosphorylation of Gal83 inhibits SnRK1 activity [15]. Phosphorylation of Gal83 by Adi3^{S212D} showed a twofold increase in Gal83 phosphorylation over wild-type Adi3 (Fig. 5A, compare Lanes 2 and 3), but did not phosphorylate Gal83 as strongly as Adi3^{S539D} (Fig. 5A, compare Lanes 3 and 4). The double phosphomimetic mutant Adi3$^{S212D/S539D}$ showed a large fourteen fold increase in Gal83 phosphorylation over wild-type Adi3 (Fig. 5A, compare Lanes 2 and 5), and had more Gal83 phosphorylation than either single phosphomimetic mutant (Fig. 5A, compare Lanes 3, 4. 5). This would suggest that phosphorylation of Ser212 contributes to Adi3 substrate phosphorylation.

Our data indicates there is an additional *Sl*Pdk1 phosphorylation site(s) on Adi3 other than Ser212 and Ser539 (Fig. 4A), suggesting this additional phosphorylation site(s) may be required for full phosphorylation of substrates by Adi3. This was tested by comparing the ability of Adi3$^{S212D/S539D}$ and *Sl*Pdk1 phosphorylated wild-type Adi3 to phosphorylate Gal83. For this assay, one sample contained Adi3$^{S212D/S539D}$ incubated with Gal83 as in Fig. 5A, while in another wild-type Adi3 was incubated first with *Sl*Pdk1 so that Adi3 would be fully phosphorylated and then Gal83 was added to the assay. The results showed Adi3$^{S212D/S539D}$ phosphorylated Gal83 to a similar level as seen previously (Fig. 5B, Lane 5), *Sl*Pdk1 could not phosphorylate Gal83 (Fig. 5B, Lane 6), and the pre-*Sl*Pdk1-phosphorylated Adi3 phosphorylated Gal83 to roughly the same level as Adi3$^{S212D/S539D}$ (Fig. 5B, Lane 7). The level of *Sl*Pdk1 phosphorylation of Adi3^{K337Q} was not affected by the incubation with Gal83 (Fig. 5B, Lane 8). This would indicate that *Sl*Pdk1 phosphorylation of both Adi3 Ser212 and Ser539 is sufficient for full Gal83 phosphorylation and that any additional

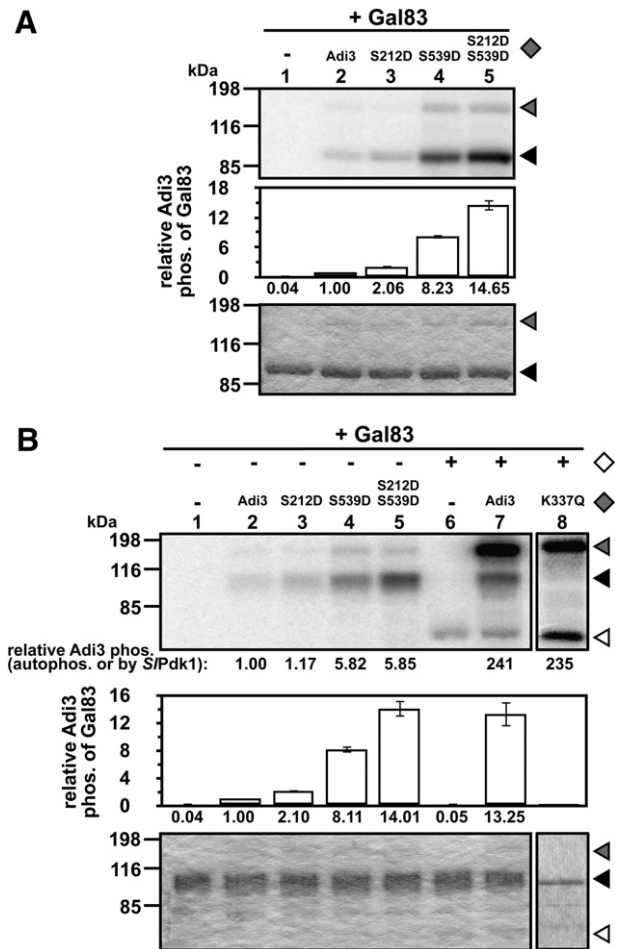**Fig. 5.** Activation of Adi3 kinase activity toward Gal83 through Ser212 and Ser539 phosphorylation. In A and B, the indicated proteins were incubated in an in vitro kinase assay with γ-[^{32}P]ATP. Top panel, phosphorimage; bottom panel, coomassie stained gel. Middle panel, quantification of Gal83 phosphorylation by Adi3 from at least 3 independent assays. Average value is shown under each column. Error bars indicate standard error. Gray diamond, form of MBP-Adi3 used in assay; open diamond, presence or absence of *Sl*Pdk1-6His. Gray, black, and open triangles, location of MBP-Adi3, MBP-Gal83, and *Sl*Pdk1-6His, respectively. The following amounts of each protein were used in the assay: *Sl*Pdk1-6His, 0.2 μg; MPB-Adi3, 0.4 μg; MBP-Gal83, 2 μg. (A) The Adi3$^{S212D/S539D}$ phosphomimetic mutant has increased kinase activity toward Gal83 compared to the single S212D and S539D phosphomimetic mutants. (B) Mutating either Ser212 or Ser539 to the phosphomimetic Asp increases Adi3 phosphorylation of Gal83. The double Adi3$^{S212D/S539D}$ phosphomimetic mutant protein has similar activity on Gal83 as Adi3 that has been fully phosphorylated by *Sl*Pdk1.

*Sl*Pdk1 phosphorylation sites on Adi3 do not significantly contribute to Gal83 phosphorylation.

4. Discussion

The data presented here identifies a second *Sl*Pdk1 phosphorylation site in Adi3, Ser212, that is required for full phosphorylation of the Gal83 substrate. Initially, we identified Ser212 by comparison with AGC1-3, the *Arabidopsis* sequence homologue to Adi3, and subsequently phosphorylation of Ser212 was identified by MS/MS. AGC1-3 has yet to be fully characterized in terms of cell death regulation, cellular localization, and substrate identification in order to confirm or deny it as a functional homologue of Adi3. While experiments of this nature are underway in our laboratory, we have not been successful in obtaining a T-DNA knockout line of AGC1-3, suggesting that a homozygous knockout of AGC1-3 may be lethal (not shown). This would support, but is not conclusive of a function for AGC1-3 similar to Adi3 in cell death suppression. Identification of AGC1-3 substrates would also help to gauge the function of this kinase. Experiments are currently ongoing toward this end. Once

J.W. Gray et al. / Biochimica et Biophysica Acta 1834 (2013) 1099–1106

AGC1-3 substrates are identified it will be of importance to test the contribution of Ser269 phosphorylation toward substrate phosphorylation for comparison with Adi3.

We also observed that the Ala mutation of AGC1-3 activation site (S596) eliminated autophosphorylation activity (Fig. 2B), while we have previously seen that the Adi3 activation site Ala mutation (S539A) does not eliminate autophosphorylation [7,14]. Differences in the effects of activation site Ala mutation in mammalian AGC kinases also range from inactivation to no effect on catalytic activity. For example, the activation site Ala mutations in PKCα and β isotypes produce an inactive protein, while in the PKCδ isotype the activation site Ala mutation maintains activity [27,28]. Thus, it appears that the plant AGC kinases contain many of the properties that have been seen in mammalian AGC kinases.

Our data also indicates there is an additional Pdk1 phosphorylation site(s) on Adi3 that accounts for approximately 10% of the total Pdk1 phosphorylation. Given the difficulty we have experienced in identifying Adi3 peptides by MS/MS, it seems other conventional methods such as Ala scanning mutagenesis and/or phosphopeptide mapping may be useful in this effort. Since our studies have shown that Ser539 and Ser212 are required for full substrate phosphorylation by Adi3, any additional Pdk1 phosphorylation sites on Adi3 may be involved in stabilizing the Adi3 protein, controlling Adi3 autophosphorylation, or regulating phosphorylation of substrates other than Gal83. It should also be noted that it still needs to be determined if these Adi3 residues are phosphorylated by Pdk1 *in planta* and if they have the same function in vivo as we have shown here by in vitro assays.

It is interesting to note the differences seen here for a plant AGC kinase compared to mammalian AGC kinases. The three main phosphorylation sites found on mammalian AGC kinases (activation site, PIF site, turn motif site) are all phosphorylated by different kinases and each has a different role in AGC kinase regulation [1,9]. In the case of plants, or at least for Adi3 and AGC1-3, it appears that Pdk1 is responsible for the multiple phosphorylation events on AGC kinases and at least two of these are required for full kinase activity on substrates. It will be of importance to determine all Pdk1 phosphorylation sites on Adi3 and determine their roles in activity or conformation stabilization.

Acknowledgements

Appendix A. Supplementary data

Supplementary data to this article can be found online at http://dx.doi.org/10.1016/j.bbapap.2013.03.006.

References

[1] L.R. Pearce, D. Komander, D.R. Alessi, The nuts and bolts of AGC protein kinases, Nat. Rev. Mol. Cell Biol. 11 (2010) 9–22.

[2] A.V. Garcia, M. Al-Yousif, H. Hirt, Role of AGC kinases in plant growth and stress responses, Cell. Mol. Life Sci. 69 (2012) 3259–3267.

[3] L. Bögre, L. Okresz, R. Henriques, R.G. Anthony, Growth signalling pathways in *Arabidopsis* and the AGC protein kinases, Trends Plant Sci. 8 (2003) 424–431.

[4] H. Zegzouti, W. Li, T.C. Lorenz, M. Xie, C.T. Payne, K. Smith, S. Glenny, G.S. Payne, S.K. Christensen, Structural and functional insights into the regulation of *Arabidopsis* AGC VIIIa kinases, J. Biol. Chem. 281 (2006) 35520–35530.

[5] J.R. Bayascas, Pdk1: the major transducer of PI 3-kinase actions, Curr. Top. Microbiol. Immunol. 346 (2010) 9–29.

[6] M. Frödin, T.L. Antal, B.A. Dummler, C.J. Jensen, M. Deak, S. Gammeltoft, R.M. Biondi, A phosphoserine/threonine-binding pocket in AGC kinases and Pdk1 mediates activation by hydrophobic motif phosphorylation, EMBO J. 21 (2002) 5396–5407.

[7] T.P. Devarenne, S.K. Ekengren, K.F. Pedley, G.B. Martin, Adi3 is a Pdk1-interacting AGC kinase that negatively regulates plant cell death, EMBO J. 25 (2006) 255–265.

[8] R.M. Biondi, Phosphoinositide-dependent protein kinase 1, a sensor of protein conformation, Trends Biochem. Sci. 29 (2004) 136–142.

[9] C. Hauge, T.L. Antal, D. Hirschberg, U. Doehn, K. Thorup, L. Idrissova, K. Hansen, O.N. Jensen, T.J. Jorgensen, R.M. Biondi, M. Frodin, Mechanism for activation of the growth factor-activated AGC kinases by turn motif phosphorylation, EMBO J. 26 (2007) 2251–2261.

[10] R. Dettori, S. Sonzogni, L. Meyer, L.A. Lopez-Garcia, N.A. Morrice, S. Zeuzem, M. Engel, A. Piiper, S. Neimanis, M. Frodin, R.M. Biondi, Regulation of the interaction between protein kinase c-related protein kinase 2 (PRK2) and its upstream kinase, 3-phosphoinositide-dependent protein kinase 1 (PDK1), J. Biol. Chem. 284 (2009) 30318–30327.

[11] R.G. Anthony, R. Henriques, A. Helfer, T. Meszaros, G. Rios, C. Testerink, T. Munnik, M. Deak, C. Koncz, L. Bögre, A protein kinase target of a PDK1 signalling pathway is involved in root hair growth in *Arabidopsis*, EMBO J. 23 (2004) 572–581.

[12] R.G. Anthony, S. Khan, J. Costa, M.S. Pais, L. Bögre, The *Arabidopsis* protein kinase PTI1-2 is activated by convergent phosphatidic acid and oxidative stress signaling pathways downstream of PDK1 and OXI1, J. Biol. Chem. 281 (2006) 37536–37546.

[13] H. Zegzouti, R.G. Anthony, N. Jahchan, L. Bogre, S.K. Christensen, Phosphorylation and activation of PINOID by the phospholipid signaling kinase 3-phosphoinositide-dependent protein kinase 1 (PDK1) in *Arabidopsis*, Proc. Natl. Acad. Sci. U. S. A. 103 (2006) 6404–6409.

[14] M.J. Ek-Ramos, J. Avila, C. Cheng, G.B. Martin, T.P. Devarenne, The T-loop extension of the tomato protein kinase AvrPto-dependent Pto-interacting protein 3 (Adi3) directs nuclear localization for suppression of plant cell death, J. Biol. Chem. 285 (2010) 17584–17594.

[15] J. Avila, O.G. Gregory, D. Su, T.A. Deeter, S. Chen, C. Silva-Sanchez, S. Xu, G.B. Martin, T.P. Devarenne, The β-subunit of the SnRK1 complex is phosphorylated by the plant cell death suppressor Adi3, Plant Physiol. 159 (2012) 1277–1290.

[16] M. Deak, A. Casamayor, R.A. Currie, C.P. Downes, D.R. Alessi, Characterisation of a plant 3-phosphoinositide-dependent protein kinase-1 homologue which contains a pleckstrin homology domain, FEBS Lett. 451 (1999) 220–226.

[17] J. Sheffield, N. Taylor, C. Fauquet, S. Chen, The cassava (*Manihot esculenta* Crantz) root proteome: protein identification and differential expression, Proteomics 6 (2006) 1588–1598.

[18] E.A. Golemis, I. Serebriiskii, R.L. Finley Jr., M.G. Kolonin, J. Gyuris, R. Brent, Interaction trap/two-hybrid system to identify interacting proteins, in: F.M. Ausubel, R. Brent, R.E. Kingston, D.D. Moore, J.G. Seidman, J.A. Smith, K. Struhl (Eds.), Curr. Protoc. Mol. Biol., John Wiley & Sons, Inc., New York, 2008, pp. 20.1.1–20.1.35.

[19] L. Demmel, M. Beck, C. Klose, A.L. Schlaitz, Y. Gloor, P.P. Hsu, J. Havlis, A. Shevchenko, E. Krause, Y. Kalaidzidis, C. Walch-Solimena, Nucleocytoplasmic shuttling of the Golgi phosphatidylinositol 4-kinase Pik1 is regulated by 14-3-3 proteins and coordinates Golgi function with cell growth, Mol. Biol. Cell 19 (2008) 1046–1061.

[20] A.C.N. Dittrich, T.P. Devarenne, An ATP analog-sensitive version of the tomato cell death suppressor protein kinase Adi3 for use in substrate identification, Biochim. Biophys. Acta 1824 (2012) 269–273.

[21] N.G. Halford, S. Hey, D. Jhurreea, S. Laurie, R.S. McKibbin, M. Paul, Y. Zhang, Metabolic signalling and carbon partitioning: role of Snf1-related (SnRK1) protein kinase, J. Exp. Bot. 54 (2003) 467–475.

[22] N.G. Halford, S.J. Hey, Snf1-related protein kinases (SnRKs) act within an intricate network that links metabolic and stress signalling in plants, Biochem. J. 419 (2009) 247–259.

[23] K.I. Mitchelhill, B.J. Michell, C.M. House, D. Stapleton, J. Dyck, J. Gamble, C. Ullrich, L.A. Witters, B.E. Kemp, Posttranslational modifications of the 5′-AMP-activated protein kinase β1 subunit, J. Biol. Chem. 272 (1997) 24475–24479.

[24] O. Vincent, M. Carlson, Gal83 mediates the interaction of the Snf1 kinase complex with the transcription activator Sip4, EMBO J. 18 (1999) 6672–6681.

[25] O. Vincent, R. Townley, S. Kuchin, M. Carlson, Subcellular localization of the Snf1 kinase is regulated by specific β subunits and a novel glucose signaling mechanism, Genes Dev. 15 (2001) 1104–1114.

[26] S.M. Warden, C. Richardson, J. O'Donnell Jr., D. Stapleton, B.E. Kemp, L.A. Witters, Post-translational modifications of the β-1 subunit of AMP-activated protein kinase affect enzyme activity and cellular localization, Biochem. J. 354 (2001) 275–283.

[27] D.B. Parekh, W. Ziegler, P.J. Parker, Multiple pathways control protein kinase C phosphorylation, EMBO J. 19 (2000) 496–503.

[28] L. Stempka, A. Girod, H.J. Muller, G. Rincke, F. Marks, M. Gschwendt, D. Bossemeyer, Phosphorylation of protein kinase Cd (PKCd) at threonine 505 is not a prerequisite for enzymatic activity. Expression of rat PKCd and an alanine 505 mutant in bacteria in a functional form, J. Biol. Chem. 272 (1997) 6805–6811.

Peptides identified by MS, alternately highlighted in <mark>yellow</mark> and <mark>green</mark>, cover 345 residues giving 49% coverage of the Adi3 protein. Peptide with Ser212 phosphorylation identified by targeted MS highlighted in <mark>orange</mark>.

MERIPEVRESTRQFPIGAKVAHTFSTSKKEVGIRGFRDFDLAIPIQTW
KGKTSYQEEEDLMVDAGTIKRSDDSLEDSGSTSFHGASHPPEPVDTDL
MRPVYVPIGQNKADGKCLVKNVSLKGPFLDDLSIRMPNVKPSPSLLSP
AESLVEEPNDLGVISSPFTVPRPSQNTETSLPPDSEEKECIWDASLPP
SGNVSPLSSIDSTGVVRSMSIVNSCTSTYRSDVLMSDGMLSVDRNYES
TKGSIRGDSLESGKTSLSRASDSSGLSDDSNWSNITGSANKPHKGNDP
RWKAILAIRARDGILGMSHFKLLKRLGCGDIGSVYLSELSGTRCYFAM
KVMDKASLASRKKLTRAQTEREILQLLDHPFLPTLYTHFETDRFSCLV
MEYCPGGDLHTLRQRQPGKHFSEYAARFYAAEVLLALEYLHMLGVVYR
DLKPENVLVRDDGHIMLSDFDLSLRCAVSPTLIRISSDDPSKRGAAFC
VQPACIEPTTVCMQPACFLPRLFPQKSKKKTPKPRADSGFQANSMPEL
VAEPTSARSMSFVGTHEYLAPEIIKGEGHGSAVDWWTFGIFLHELLYG
KTPFKGSGNRATLFNVVGQQLKFPDSPATSYASRDLIRGLLVKEPQNR
LGVKRGATEIKQHPFFEGVNWALIRCSTPPEVPRPVEPDYPAKYGQVN
PVGVGNTSKRVVGADAKSGGKYLDFEFF

Potential Pdk1 phosphorylation sites on Adi3 identified by MS here: <mark>S119</mark>, <mark>S518</mark>

Pdk1 phosphorylation site on Adi3 previously identified as well as here by MS: <mark>S539</mark>

Pdk1 phosphorylation site identified by homology with *At*AGC1-3 and MS: <mark>S212</mark>

Supplemental Figure 1. **Adi3 peptide MS coverage and Pdk1 phosphorylation site identification**. The Adi3 protein sequence showing peptides identified by MS, alternately highlighted in yellow and green, from Pdk1 phosphorylated Adi3 giving 49% coverage of the total Adi3 protein. Phosphorylation sites identified by MS or homology to *At*AGC1-3 are highlighted as indicated.

Ser119 phosphorylation
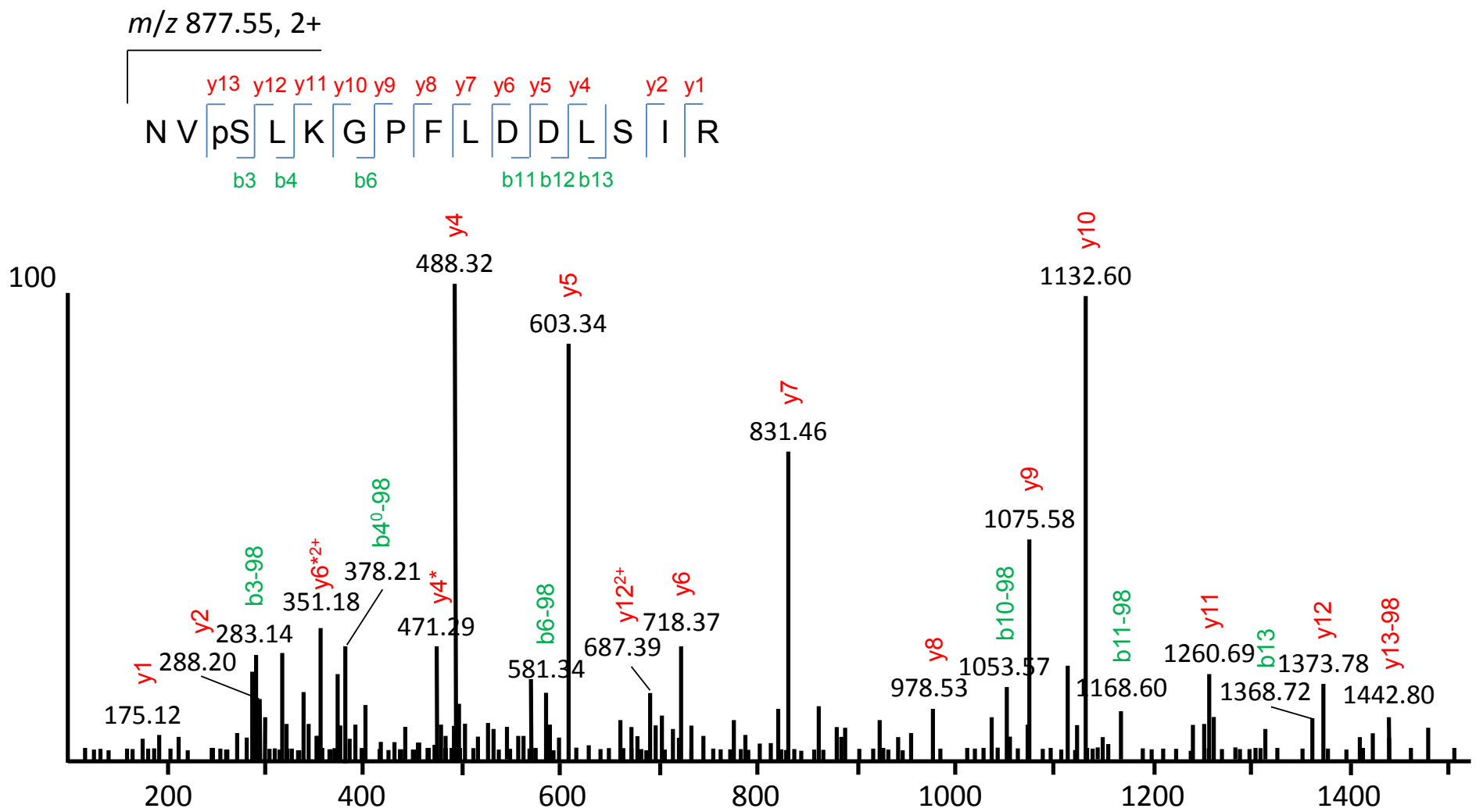
Supplemental Figure 2. MS/MS spectra of Pdk1 phosphorylated Adi3 peptide with Ser119 phosphorylation. * indicates loss of NH_3 and ^{0} indicates loss of H_2O.

Ser518 phosphorylation

m/z 1129.50, 2+

A D pS G F Q A N S M P E L V A E P T S A R
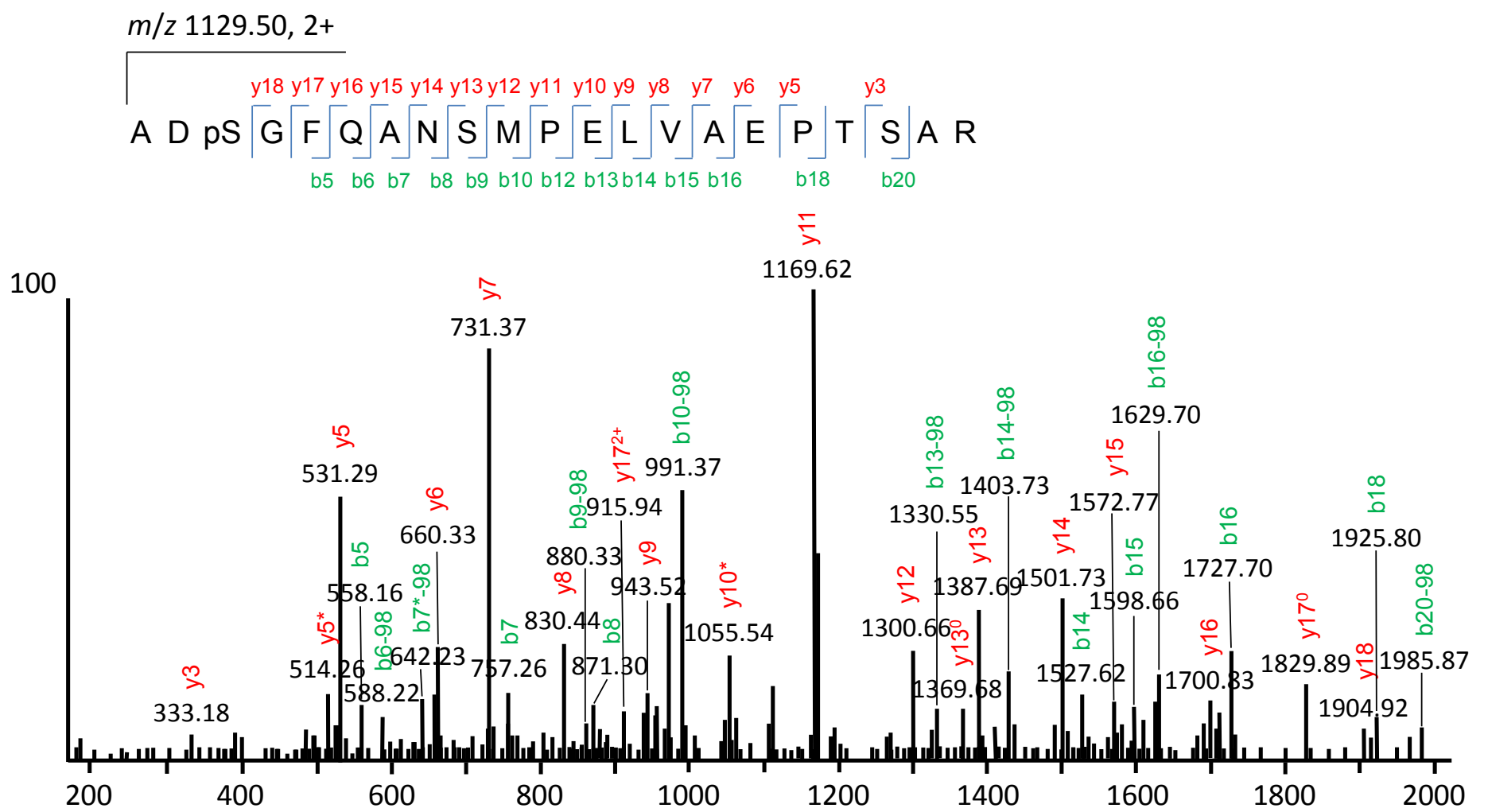
Supplemental Figure 3. MS/MS spectra of Pdk1 phosphorylated Adi3 peptide with Ser518 phosphorylation. * indicates loss of NH_3 and [0] indicates loss of H_2O.
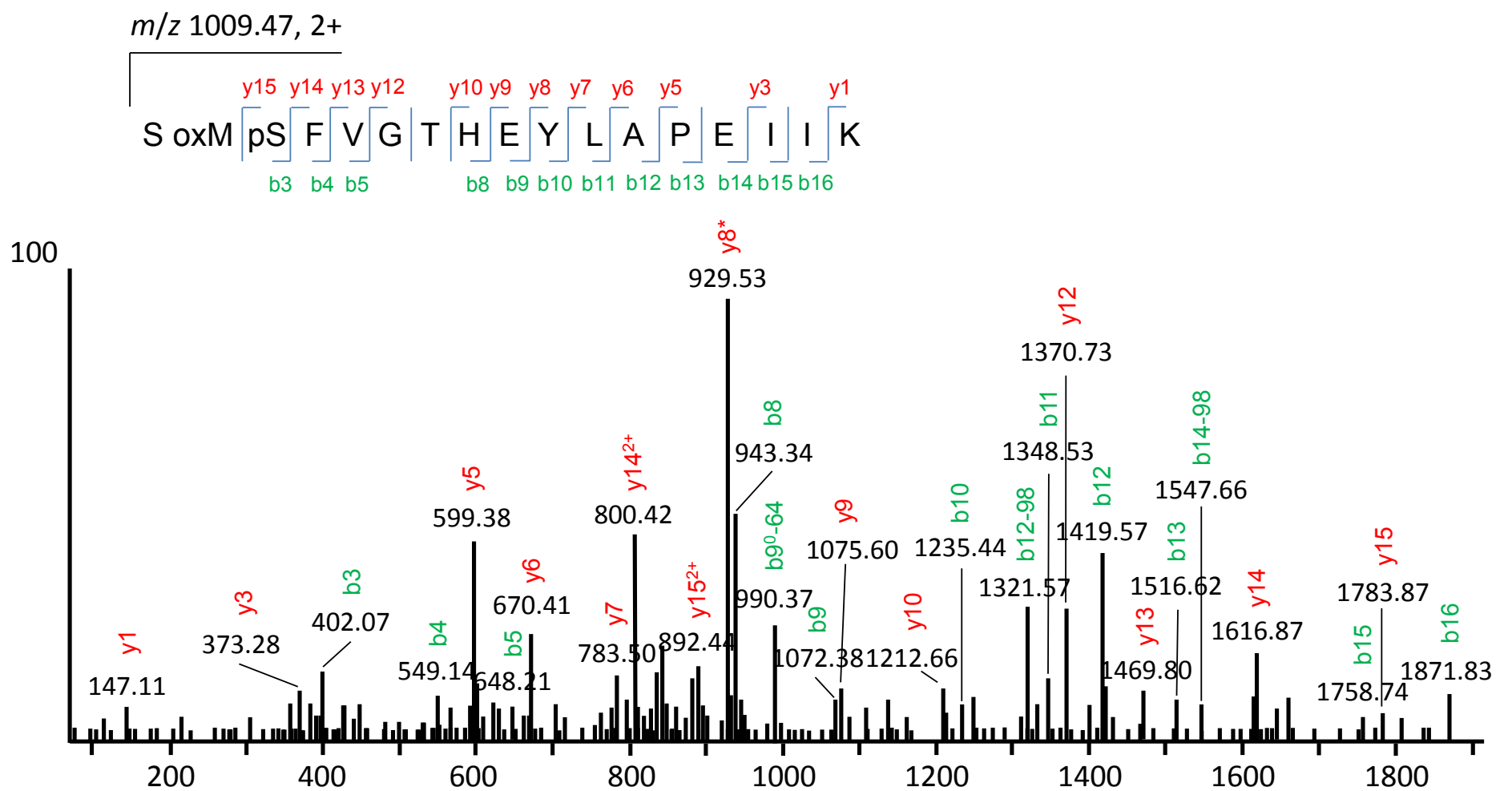
Supplemental Figure 4. MS/MS spectra of Pdk1 phosphorylated Adi3 peptide with Ser539 phosphorylation. * indicates loss of NH_3, ^{0} indicates loss of H_2O, and ox stands for oxidized.

```
At2g44830   MLEMERVAELKRLPSKGPVSGHLSRRPYLDFETRDAPGMHLESLRERAARYNTGRSVNPT 60
Adi3        ---MERIPEVRES------------------TRQFP--------------------- 15
                **** *.*::.                        **: *

At2g44830   TTLGRELSQVLNVHREDMMMTQFGGNMNDFQEFEPVVSSVRTMKAKYPLLEIEEIGAADD 120
Adi3        --IGAKVAHTFSTSKK-----EVG--IRGFRDFDLAIP-IQTWKGKTSYQEEDLMVDAG 65
              :*  :::::... :  :.*  :...*::*: .:. ::* *.*  .  *  *:: .  .

At2g44830   DVTCKGSNDMSEEAGSSSFRGVSHPPEPDDMDLITTVYVPISEKNKPDSVCLMKSMSTTK 180
Adi3        --TIKRSDDSLEDSGSTSFHGASHPPEPVDTDLMRPVYVPIGQ-NKADGKCLVKNVSLK 121
              *  * *:*  *::**:**:*.****** * **: .*****.: **.*. **:*.:*   *

At2g44830   GPFIEDISLCVPPKKPSPRVLSPAESIVEEP---ATSLSPFSVARASQNTENSLLPPDSD 237
Adi3        GPFLDDLSIRMPNVKPSPSLLSPAESLVEEPNDLGVISSPFTVPRPSQNTETSLPPDSEE 181
            ***::*:*: :*    **** :******:****    ..   ***:*.*.*****.** * ..:

At2g44830   KECVWDASLPPSTNVSPHSSSVESMNLARAMSIANSSSAT--STTQRSDVVLSMDKNYFD 295
Adi3        KECIWDASLPPSGNVSPLSS-IDSTGVVRSMSIVNSCTSTYRSDVLMSDGMLSVDRNYES 240
            ***:********* **** ** ::* .:.*:***.**.::*  *  ** :**:*:** .

At2g44830   RSISMVLDSFESTKTSASRASDSSGLSEESSWSNFTGSLNKPHKGNDPWWNAILAIRTRD 355
Adi3        TKGSIRGDSLESGKTSLSRASDSSGLSDDSNWSNITGSANKPHKGNDPRWKAILAIRARD 300
            . *:    **:** *** **********::*.***:*** ********* *:******:**

At2g44830   GILGMSHFKLLKRFGCGDIGSVYLAELSGTRCHFAVKVMDKASLEDRKKLNRAQTERDIL 415
Adi3        GILGMSHFKLLKRLGCGDIGSVYLSELSGTRCYFAMKVMDKASLASRKKLTRAQTEREIL 360
            *************:***********:*******:**:********  .****.*******:*

At2g44830   QLLDHPFLPTLYTHFETDRFSCLVMEYCPGGDLHTLRQRQPGKHFSEYAARFYAAEVLLA 475
Adi3        QLLDHPFLPTLYTHFETDRFSCLVMEYCPGGDLHTLRQRQPGKHFSEYAARFYAAEVLLA 420
            ***********************************************************

At2g44830   LEYLHMLGVVYRDLKPENVLVRDDGHIMLSDFDLSLRCAVSPTLIKTFDSDPSRRG-AFC 534
Adi3        LEYLHMLGVVYRDLKPENVLVRDDGHIMLSDFDLSLRCAVSPTLIRISSDDPSKRGAAFC 480
            *************************************************:  ..***:** ***

At2g44830   VQPACMEPTSACIIQPSCFLPRSIFPNKNKKNKSRKTQADFFKSHSGSLPELVAEPN-TR 593
Adi3        VQPACIEPTTVC-MQPACFLPR-LFPQKSKKKTPKPRADSGFQANS--MPELVAEPTSAR 536
            *****:***.* :**:***** :**:*.**:..:   . *::* :*******. :*

At2g44830   SMSFVGTHEYLAPEIIKGEGHGSAVDWWTFGIFVHELLYGKTPFKGSGNRATLFNVVGEQ 653
Adi3        SMSFVGTHEYLAPEIIKGEGHGSAVDWWTFGIFLHELLYGKTPFKGSGNRATLFNVVGQQ 596
            *********************************:*************************:*

At2g44830   LKFPESPATSYAGRDLIQALLVKDPKNRLGTKRGATEIKQHPFFEGVNWALIRCSTPPEV 713
Adi3        LKFPDSPATSYASRDLIRGLLVKEPQNRLGVKRGATEIKQHPFFEGVNWALIRCSTPPEV 656
            ****:*******.****:.****:*:****.***************************

At2g44830   PRQMETEPPPKYGPIDPVGFGSNSKRMMGPPAVSAAAADTKSGGKFLDFEFF 765
Adi3        PRPVEPDYPAKYGQVNPVGVGNTSKRVVG--------ADAKSGGKYLDFEFF 700
            ** :*.: *.*** ::***.*..***.*..**::*      **:*****:******
```

Supplemental Figure 5. **Protein alignment of Adi3 and AGC1-3 (At2g44830)**. Proteins were aligned using ClusalW. Phosphorylated amino acids identified by MS here highlighted in blue; Pdk1 phosphor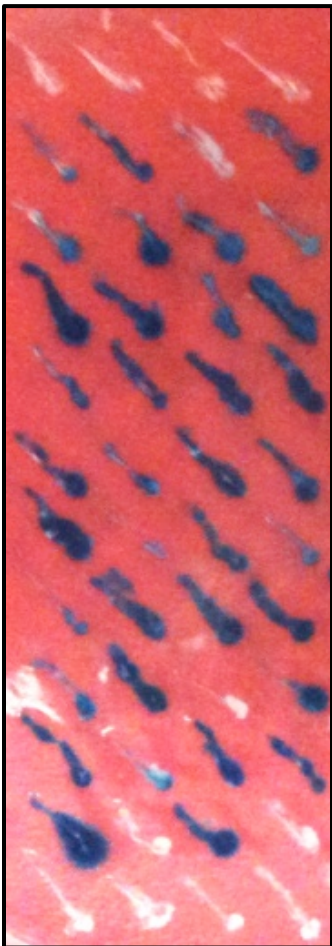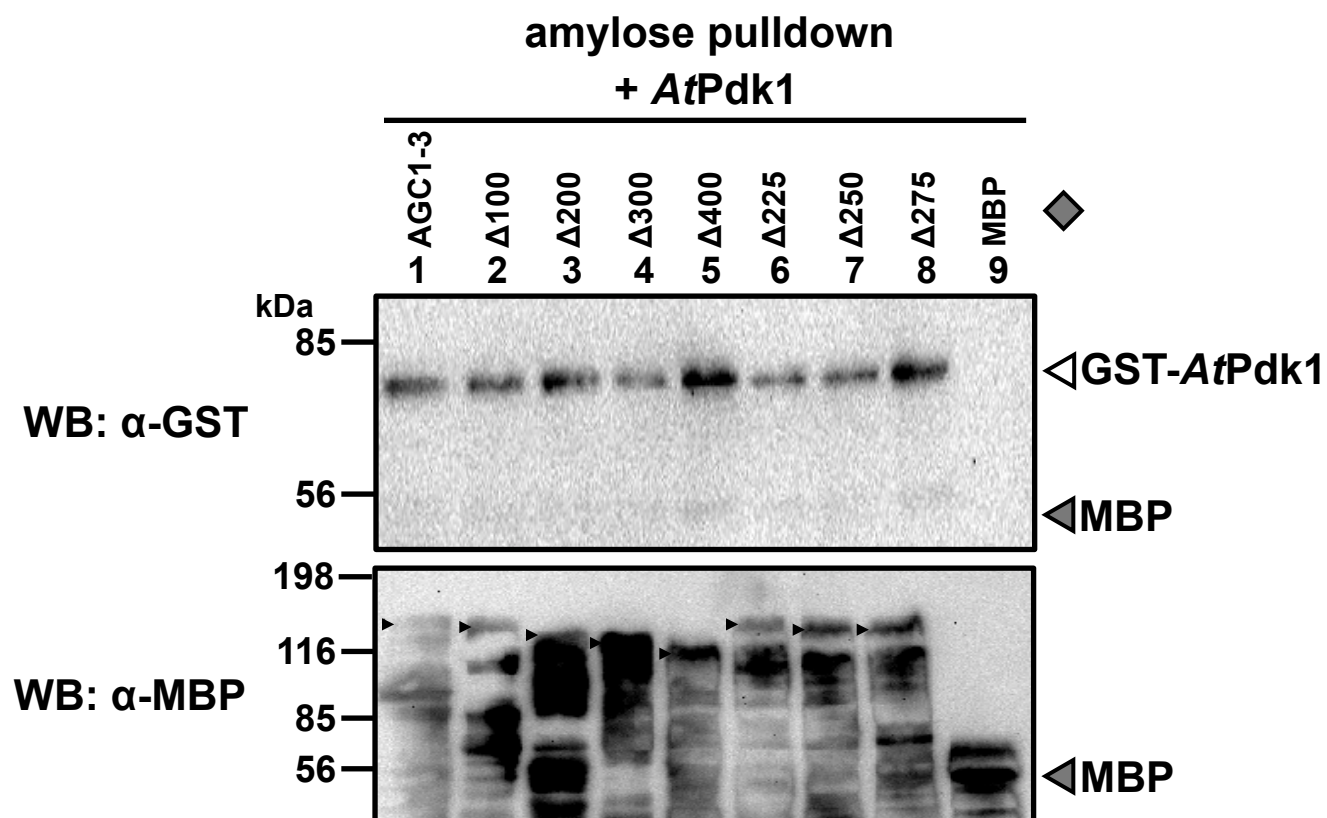ylation site identified by homology with *At*AGC1-3 and MS highlighted in purple; Pdk1 phosphorylation site on Adi3 previously identified as well as here by MS highlighted in red; Lysine residue involved in ATP binding highlighted in green; PIF-binding pocket highlighted in pink with last residue within kinase domain highlighted in pink; T-loop extension highlighted in orange; PIF highlighted in yellow.

Bait	**Prey**	X-Gal	sample
AtPdk1	**Dorsal**		1
***At*Pdk1**	**AGC1-3**		2
AGC1-3	***At*Pdk1**		3
***At*Pdk1**	**AGC1-3^{K392Q}**		4
***At*Pdk1**	**AGC1-3^{S269A}**		5
***At*Pdk1**	**AGC1-3^{S596A}**		6
***At*Pdk1**	**AGC1-3^{S269D}**		7
***At*Pdk1**	**AGC1-3^{S596D}**		8
***At*Pdk1**	**AGC1-3$^{S269A/S596A}$**		9
***At*Pdk1**	**AGC1-3$^{S269D/S596D}$**		10
***At*Pdk1^{K73Q}**	**AGC1-3**		11
***At*Pdk1**	**AGC1-3$^{\Delta PIF}$**		12

Supplemental Figure 6. **AGC1-3 yeast two-hybrid interactions with *At*Pdk1**. The indicated bait and prey constructs were tested in the Y2H assay for expression of the *lacZ* gene on X-Gal plates (blue = interaction). The *Drosophila* protein Dorsal was used as negative control and indicate that the *At*Pdk1/Adi3 interaction is specific.

amylose pulldown
+ *At*Pdk1

AGC1-3 | Δ100 | Δ200 | Δ300 | Δ400 | Δ225 | Δ250 | Δ275 | MBP

1 2 3 4 5 6 7 8 9

kDa

85

WB: α-GST

56

◁GST-*At*Pdk1

◁MBP

198

116

WB: α-MBP

85

56

◁MBP

Supplemental Figure 7. **AGC1-3 N-terminal truncations interact with *At*Pdk1**. The indicated N-terminal truncated MBP-AGC1-3$^{K337Q/S596A}$ proteins were incubated with GST-*At*Pdk1 or MBP for 1 hr at 4°C and the MBP-tagged proteins pulled down with amylose resin. Each pull-down was split into two equal fractions and analyzed for the presence of GST-Pdk1 by α-GST western blot (top panel) and the N-terminal truncated MBP-AGC1-3$^{K337Q/S596A}$ proteins by α-MBP western blot (bottom panel). Gray diamond, truncated form of AGC1-3 in the kinase inactive MBP-AGC1-3$^{K392Q/S595A}$ background used in assay. White and gray triangles, location of GST-*At*Pdk1 and MBP. Small black triangles on α-MBP western blot (bottom panel) indicate position of N-terminal truncated MBP-AGC1-3$^{K337Q/S596A}$ proteins.
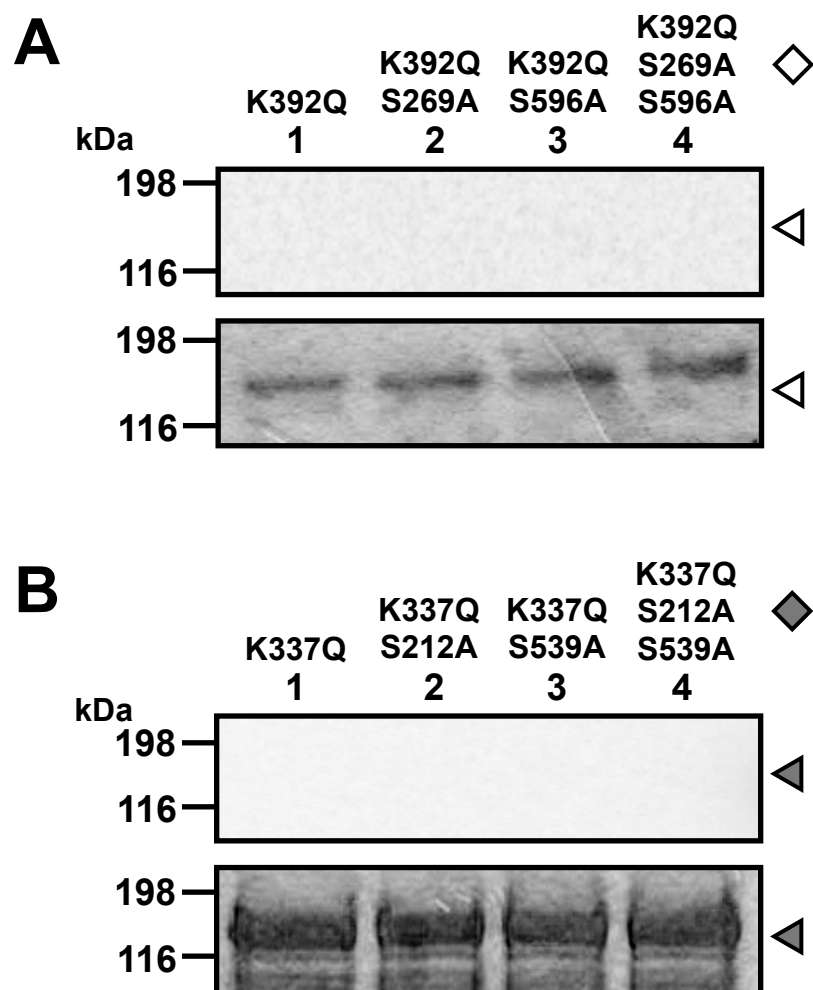
Supplemental Figure 8. **Autophosphorylation of the AGC1-3 S269A and S596A mutants in the kinase-inactive K392Q background and Adi3 S212A and S539A mutants in the kinase-inactive K337Q background**. In A and B, the indicated proteins were incubated in an *in vitro* kinase assay with γ-[^{32}P]ATP. Top panel, phosphorimage; bottom panel, Coomassie stained gel. Gray and white diamonds, form of MBP-Adi3 or MPB-AGC1-3 used in assay, respectively. Gray and white triangles, location of MBP-Adi3 or MPB-AGC1-3, respectively . 5 µg of MPB-Adi3 and 3 µg of MPB-AGC1-3 was used in the assay. **(A)** AGC1-3 autophosphorylation. **(B)** Adi3 autophosphorylation.

Ser212 phosphorylation
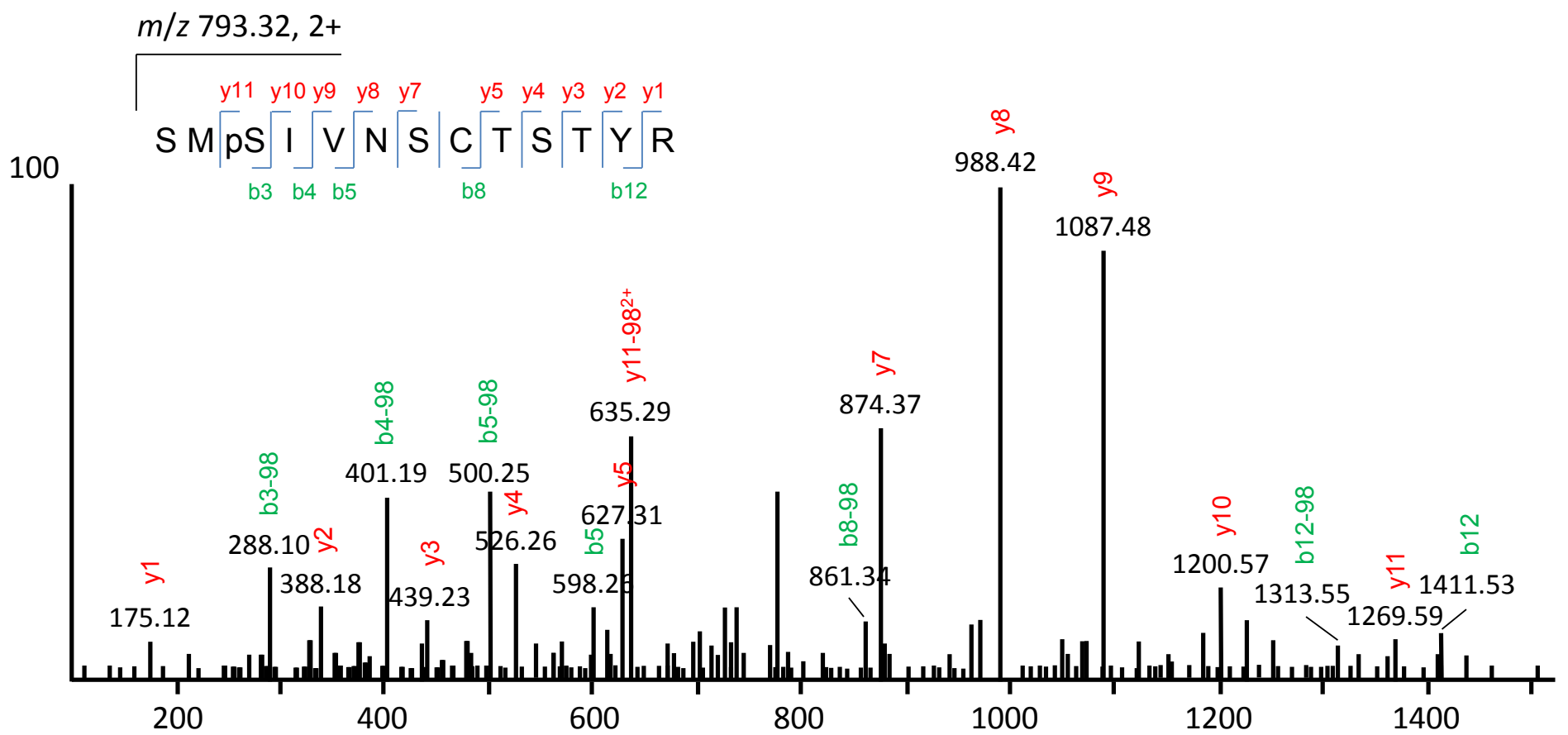
Supplemental Figure 9.   MS/MS spectra of Pdk1 phosphorylated Adi3 peptide with Ser212 phosphorylation.

Supplemental Table 1. Primers used in this study.

Gene	Primer Name	Purpose	Direction	Restriction site	Sequence
Adi3	S119A	Mutagenesis	Forward		5'- CTGGTGAAAAACGTA**GCA**TTGAAGGGTCCTTTC-3'
Adi3	S119A	Mutagenesis	Reverse		5'- GAAAGGACCCTTCAA**TGC**TACGTTTTTCACCAG-3'
Adi3	S119D	Mutagenesis	Forward		5'- CTGGTGAAAAACGTA**GAC**TTGAAGGGTCCTTTC-3'
Adi3	S119D	Mutagenesis	Reverse		5'- GAAAGGACCCTTCAA**GTC**TACGTTTTTCACCAG-3'
Adi3	S212A	Mutagenesis	Forward		5'- GTTGTGAGATCTATG**GCA**ATTGTCAACAGTTGC-3'
Adi3	S212A	Mutagenesis	Reverse		5'- GCAACTGTTGACAAT**TGC**CATAGATCTCACAAC-3'
Adi3	S212D	Mutagenesis	Forward		5'-GTTGTGAGATCTATG**GAC**ATTGTCAACAGTTGC-3'
Adi3	S212D	Mutagenesis	Reverse		5'-GCAACTGTTGACAAT**GTC**CATAGATCTCACAAC-3'
Adi3	S518A	Mutagenesis	Forward		5'- CCTAAGCCTCGAGCTGAT**GCA**GGGTTTCAAGCTAATTCAATGCC-3'
Adi3	S518A	Mutagenesis	Reverse		5'- GGCATTGAATTAGCTTGAAACCC**TGC**ATCAGCTCGAGGCTTAGG-3'
Adi3	S518D	Mutagenesis	Forward		5'- CCTAAGCCTCGAGCTGAT**GAT**GGGTTTCAAGCTAATTCAATGCC-3'
Adi3	S518D	Mutagenesis	Reverse		5'- GGCATTGAATTAGCTTGAAACCC**ATC**ATCAGCTCGAGGCTTAGG-3'
Adi3	S651A	Mutagenesis	Forward		5'- GCTCTAATACGTTGC**GCA**ACACCACCTGAAGTG-3'
Adi3	S651A	Mutagenesis	Reverse		5'- CACTTCAGGTGGTGT**TGC**GCAACGTATTAGAGC-3'
Adi3	S651D	Mutagenesis	Forward		5'- GCTCTAATACGTTGC**GAT**ACACCACCTGAAGTG-3'
Adi3	S651D	Mutagenesis	Reverse		5'- CACTTCAGGTGGTGT**ATC**GCAACGTATTAGAGC-3'
Adi3	S680A	Mutagenesis	Forward		5'- GGGGTTGGCAATACC**GCA**AAAAGAGTGGTAGGG-3'
Adi3	S680A	Mutagenesis	Reverse		5'- CCCTACCACTCTTTT**TGC**GGTATTGCCAACCCC-3'
Adi3	S680D	Mutagenesis	Forward		5'- GGGGTTGGCAATACC**GAC**AAAAGAGTGGTAGGG-3'
Adi3	S680D	Mutagenesis	Reverse		5'- CCCTACCACTCTTTT**GTC**GGTATTGCCAACCCC-3'
AGC1-3	AGC1-3/EcoRIF	ORF Amplification Cloning into pEG202/pJG4-5/ pETMAL	Forward	EcoRI	5' –CAC<u>GAATTC</u>ATGCTGGAAATGGAAAGAG-3'
AGC1-3	AGC1-3/XhoIR	ORF Amplification Cloning into pEG202/pJG4-5/ pETMAL	Reverse	XhoI	5' –CAC<u>CTCGAG</u>TTAGAAAAACTCAAAGTC-3'
AGC1-3	K392Q	Mutagenesis	Forward		5' –CGATGCCATTTTGCTGTG**CAA**GTCATGGATAAAGCGTCT-3'
AGC1-3	K392Q	Mutagenesis	Reverse		5' –AGACGCTTTATCCATGAC**TTG**CACAGCAAAATGGCATCG-3'
AGC1-3	S596A	Mutagenesis	Forward		5' –CCTAACACACGGTCCATG**GCC**TTTGTTGGAACCCACGAG-3'
AGC1-3	S596A	Mutagenesis	Reverse		5' –CTCGTGGGTTCCAACAAA**GGC**CATGGACCGTGTGTTAGG-3'
AGC1-3	S596D	Mutagenesis	Forward		5' –CCTAACACACGGTCCATG**GAC**TTTGTTGGAACCCACGAG-3'
AGC1-3	S596D	Mutagenesis	Reverse		5' –CTCGTGGGTTCCAACAAA**GTC**CATGGACCGTGTGTTAGG-3'
AGC1-3	S269A	Mutagenesis	Forward		5' –TTGGCTCGGGCTATG**GCC**ATTGCTAATAGCTCT-3'
AGC1-3	S269A	Mutagenesis	Reverse		5' –AGAGCTATTAGCAAT**GGC**CATAGCCCGAGCCAA-3'
AGC1-3	S269D	Mutagenesis	Forward		5' –TTGGCTCGGGCTATG**GAC**ATTGCTAATAGCTCT-3'
AGC1-3	S269D	Mutagenesis	Reverse		5' –AGAGCTATTAGCAAT**GTC**CATAGCCCGAGCCAA-3'
AGC1-3	AGC1-3/NoPIF XhoI	Cloning into pJG4-5 without the PIF	Reverse	XhoI	5' –CAC<u>CTCGAG</u>TTAGTCTAGAAATTTACC-3'
AtPDK1-1	AtPDK1-1/EcoRIF	Cloning into pGEX/ pEG202/pJG4-5	Forward	EcoRI	5' –CAC<u>GAATTC</u>ATGTTGGCAATGGAG-3'
AtPDK1-1	AtPDK1-1/XhoIR	Cloning into pGEX/ pEG202/pJG4-5	Reverse	XhoI	5' –CAC<u>CTCGAG</u>TCAGCGGTTCTGAAGAGT-3'
AtPDK1-1	K73Q	Mutagenesis	Forward		5' –ACTGTGTATGCTTTA**CAG**ATTATGGACAAAAAG-3'
AtPDK1-1	K73Q	Mutagenesis	Reverse		5' –CTTTTTGTCCATAAT**CTG**TAAAGCATACACAGT-3'
MBP	MBP/NdeI	Cloning MBP in place of GST in pET41a	Forward	NdeI	5' –CAC<u>CATATG</u>AAAACTGAAGAAGGT-3'
MBP	MBP/SpeI	Cloning MBP in place of GST in pET41a	Reverse	SpeI	5' –CAC<u>ACTAGT</u>TGAAATCCTTCCCTC-3'